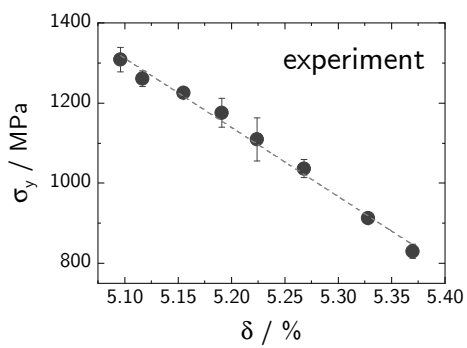


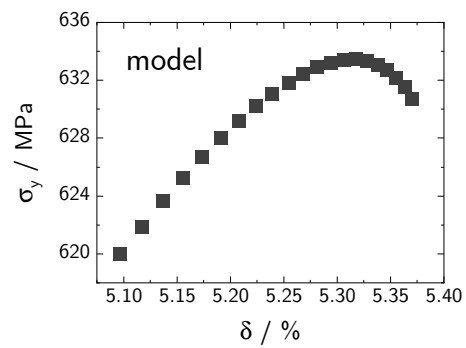
1 Graphical Abstract

2 **Breakdown of Varvenne scaling in $(\text{AuNiPdPt})_{1-x}\text{Cu}_x$ high-entropy**
3 **alloys**

4 F. Thiel, D. Utt, A. Kauffmann, K. Nielsch, K. Albe, M. Heilmaier, J. Freuden-
5 berger



VS.



6 Highlights

7 **Breakdown of Varvenne scaling in $(\text{AuNiPdPt})_{1-x}\text{Cu}_x$ high-entropy** 8 **alloys**

9 F. Thiel, D. Utt, A. Kauffmann, K. Nielsch, K. Albe, M. Heilmaier, J. Freuden-
10 berger

- 11 • $(\text{AuNiPdPt})_{1-x}\text{Cu}_x$ forms a homogeneous solid solution with deliber-
12 ately adjusted Cu concentration making it an ideal candidate to inves-
13 tigate concentration-dependent solid solution strengthening in concen-
14 trated solid solutions.
- 15 • The yield strength of $(\text{AuNiPdPt})_{1-x}\text{Cu}_x$ decreases linearly with x ,
16 while the opposite trend and non-linear scaling is expected from theory.
- 17 • The absolute values as well as the range across the Cu concentration of
18 the experimental yield strength is higher and much more pronounced
19 when compared to the theoretical prediction.

20 Breakdown of Varvenne scaling in $(\text{AuNiPdPt})_{1-x}\text{Cu}_x$
21 high-entropy alloys

22 F. Thiel^{a,b}, D. Utt^c, A. Kauffmann^d, K. Nielsch^{a,b}, K. Albe^c, M. Heilmaier^d,
23 J. Freudenberger^{a,e}

24 ^aLeibniz IFW Dresden, Helmholtzstraße 20, D-01069 Dresden, Germany

25 ^bTU Dresden, Institute of Materials Science, D-01062 Dresden, Germany

26 ^cTU Darmstadt, Institut für Materialwissenschaft, Otto-Berndt-Str. 3, D-64287

27 Darmstadt, Germany

28 ^dKarlsruhe Institute of Technology (KIT), Institute for Applied Materials,

29 Engelbert-Arnold-Straße 4, D-76131 Karlsruhe, Germany

30 ^eTU Bergakademie Freiberg, Institute of Materials Science, Gustav-Zeuner-Straße 5,

31 D-09599 Freiberg, Germany

32 **Abstract**

The compositional dependence of the yield strength σ_y has been studied for a series of polycrystalline $(\text{AuNiPdPt})_{1-x}\text{Cu}_x$ alloys by means of compression tests. σ_y is found to decrease linearly with increasing Cu concentration. This behaviour is in contradiction to the generalised theory for solid solution strengthening in concentrated solid solutions provided by Varvenne et al. [1]. A breakdown of the scaling behaviour is found as σ_y should be non-linear and slightly increasing when modifying the composition from AuNiPdPt to AuCuNiPdPt.

33 *Keywords:* high-entropy alloys, noble metals, mechanical properties,
34 solution strengthening, yield stress predictions

35 In the past decade, a new class of materials possessing advanced prop-
36 erties has attracted much interest in the field of physical metallurgy. These
37 materials are the result of an alternative design strategy; while conventional

Email address: j.freudenberger@ifw-dresden.de (J. Freudenberger)

Preprint submitted to Scripta Materialia

January 24, 2020

38 alloy design is based on one main element, there is no main element in mul-
39 ticomponent alloys which are called high-entropy alloys (HEA). The class
40 of HEA has stimulated research since its discovery back in 2004 [2, 3]. Be-
41 sides superior properties that are addressed with the HEAs in particular, the
42 phenomenon of solid solution strengthening is still under investigation [4, 5].
43 Nowadays and in what follows here, only those multi-component alloys which
44 are single-phase are called HEAs [6].

45 Up to now, there is no wholistic model to assess the effect of solid solu-
46 tion strengthening in HEAs. The development of such a model is challenging,
47 since it would need to consider contributions to the strength arising from (i)
48 lattice distortions, (ii) variations of the shear modulus as well as (iii) vari-
49 ations of the stacking fault energy. However, the latter has been proven to
50 have only minor influence on the strength [7, 8]. So far, the most compre-
51 hensive model applied for the assessment of the solid solution strengthening
52 in HEAs is that one derived by Varvenne et al. [1, 9]. This model repre-
53 sents an extension of the Labusch-type weak-pinning model [7, 1]. It clearly
54 identifies which material parameters play the major role for strengthening,
55 i.e. (i) the strength does not directly depend on the number of elements in
56 the alloy, (ii) the shear modulus or the concentration-weighted mean-square
57 misfit volume quantity are the key parameters for the determination of the
58 strength. Although being widely applied, this model bears significant draw-
59 backs. The theory assumes a random distribution of the components on the
60 lattice site, which is presumably not the case. Local chemical environments
61 as e.g. segregations, structural disorder and short-range order represent ad-
62 ditional contributions to the strength of HEAs which are not addressed in

63 the model, as recently stressed in [10].

64 AuCuNiPdPt represents a HEA, that was designed upon a combination
65 of elements whose binary phase diagrams show solubility within the entire
66 concentration range [11, 12]. Besides the quinary alloy, any quaternary com-
67 bination of Au, Cu, Ni, Pd and Pt has been proven to form a homogeneous
68 solid solution [11]. As a consequence, this system represents an ideal can-
69 didate to investigate composition-dependent solid solution strengthening in
70 concentrated solid solutions.

71 In the present article, the scaling behaviour of the yield strength σ_y and
72 the microhardness have been investigated for a series of $(\text{AuNiPdPt})_{1-x}\text{Cu}_x$
73 high-entropy alloys. Moreover, the yield strengths of this series of alloys
74 were calculated according to Refs. [1, 9] and compared to the experimental
75 results. The mentioned series has been chosen in accordance to the model
76 of solid solution strengthening with respect to the corresponding increase of
77 the strength originating from the paraelastic interaction.

78 Polycrystalline samples of $(\text{AuNiPdPt})_{1-x}\text{Cu}_x$ ($x = 0, 1, 3, 5, 7, 10, 15, 20$ at.%)
79 were prepared from pure elements by arc melting. For this purpose, x Cu
80 was added in stoichiometry to a previously prepared master alloy with the
81 nominal composition AuNiPdPt. For improving the sample homogeneity,
82 the samples were turned-over and re-melted four times prior to suction cast-
83 ing into a water-cooled copper mould with 4 mm in diameter and 75 mm
84 in length. The as-cast alloys were homogenised at 1100 °C to 1200 °C de-
85 pending on the composition for 20 h with subsequent water-quenching. The
86 proper homogenisation temperature T_h of any individual alloy has been de-
87 termined previously by differential scanning calorimetry and set to be at least

88 $T_h \simeq 0.9 T_m$, with T_m being the melting temperature of the alloy. Annealing
89 was performed in sealed fused silica ampoules under protective Ar atmo-
90 sphere. The homogenised samples were cold worked by rotary swaging at
91 room temperature up to a deformation strain of $\varphi = 0.6$ and afterwards heat
92 treated at the same temperatures mentioned above for 1 h in order to obtain
93 a fully recrystallised microstructure. Phase purity has been investigated by
94 means of X-ray diffraction (XRD) in Debye-Scherrer geometry on samples
95 with a thickness of $\leq 30 \mu\text{m}$ utilising a STOE STADI P diffractometer with
96 $\text{MoK}_{\alpha 1}$ radiation.

97 For microstructural analysis and microhardness tests, the samples were
98 prepared by a conventional metallographic procedure as described in Ref. [12].
99 Microstructural characterisation was carried out by scanning electron mi-
100 croscopy (SEM) using a FEI Helios 600i operating at 10 kV and 1.4 nA.
101 Microhardness measurements were performed with a Shimadzu HMV-2 hard-
102 ness tester operating at a load of 1.98 N. Mechanical tests were performed
103 in compression utilising an electro-mechanical Instron 8562 testing machine
104 on samples with an initial diameter d_0 of 3 mm and a height h_0 of $\lesssim 6\text{mm}$.
105 Tests were stopped when the aspect ratio approached $h_0/d_0 = 1$. An initial
106 engineering strain rate of $\dot{\epsilon} = 1 \cdot 10^{-3} \text{ s}^{-1}$ was applied.

Calculation of the yield strength as a result of solid solution strengthening has been performed according to the Varvenne model [1, 9] assuming that it can be described by an effective average matrix (“solvent”) with all atoms being embedded “solute” atoms. Here, the average matrix represents the mean properties of the HEA, while the embedded solutes account for the local chemical fluctuations [1, 13, 14]. The model has been simplified considering

only for elastic contributions, i.e. Eqs. 1-3 are used to evaluate the critical shear stress for dislocation slip τ_y as function of temperature T and strain rate $\dot{\epsilon}$:

$$\tau_y(T, \dot{\epsilon}) = \tau_{y0} \left[1 - \left(\frac{k_B T}{\Delta E_b} \ln \frac{\dot{\epsilon}_0}{\dot{\epsilon}} \right)^{\frac{2}{3}} \right], \text{ with} \quad (1)$$

$$\tau_{y0} = 0.01785 \alpha^{-\frac{1}{3}} \bar{G} \left(\frac{1 + \bar{\nu}}{1 - \bar{\nu}} \right)^{\frac{4}{3}} \left[\frac{\sum_n c_n \Delta V_n^2}{b^6} \right]^{\frac{2}{3}}, \text{ and} \quad (2)$$

$$\Delta E_b = 1.56318 \alpha^{\frac{1}{3}} \bar{G} b^3 \left(\frac{1 + \bar{\nu}}{1 - \bar{\nu}} \right)^{\frac{2}{3}} \left[\frac{\sum_n c_n \Delta V_n^2}{b^6} \right]^{\frac{1}{3}}, \quad (3)$$

with \bar{G} : average shear modulus of the matrix as calculated upon the linear rule of mixture, $\bar{\nu}$: Poisson's ratio, c_n : concentration of the alloying element n , $\Delta V_n = V_n - \bar{V}$: misfit volume, b : length of the Burgers vector, k_B : Boltzmann constant. The [input data is provided in Tab. 1](#) and the following parameters have been used: $\alpha = 0.123$, $\dot{\epsilon} = 10^{-3} \text{s}^{-1}$, $\dot{\epsilon}_0 = 10^4 \text{s}^{-1}$ in accordance with Ref. [1]. $\sum_n c_n \Delta V_n^2$ is the key misfit parameter. In the present case all elements crystallise in the same crystal structure, a homogeneous solid solution is observed and Vegard's law can be applied. Therefore, in accordance to Ref. [15] this misfit parameter can be related to:

$$\delta = \sqrt{2 \sum_n c_n \Delta V_n^2 / 9b^6}. \quad (4)$$

107 δ can also be obtained from the misfit of the lattice parameters, which would
 108 yield approximately the same result. However, this consideration [1, 15]
 109 was made for alloys where the corresponding elements have similar lattice
 110 parameters, which is not the case for the Au-Cu-Ni-Pd-Pt system. Hence,
 111 the two δ values are different but qualitatively yield the same results for the
 112 present alloy and the misfit parameter calculated on the basis of the volume

113 (c.f. Eq. 4) is used for the following discussion. Using a Taylor factor of 3.06,
114 τ_y provides the yield strength σ_y^{theo} .

115 All recrystallised $(\text{AuNiPdPt})_{1-x}\text{Cu}_x$ alloys are single-phase and crys-
116 tallise in a face-centered cubic structure (fcc, Cu-type). The corresponding
117 XRD patterns show no evidence of secondary phases as can be seen exem-
118 plarily for the $(\text{AuNiPdPt})_{97}\text{Cu}_3$ alloy in Fig. 1. This figure also depicts
119 the microstructure of the recrystallised alloys utilising SEM with backscat-
120 tered electron (BSE) imaging. The images reveal no indications of secondary
121 phases and an average grain size of 40 μm to 60 μm .

122 Rietveld refinements of the XRD patterns were utilised to determine the
123 lattice parameter a of the $(\text{AuNiPdPt})_{1-x}\text{Cu}_x$ alloys. As can be seen from
124 Fig. 2, the lattice parameter scales linearly with the Cu content. This be-
125 haviour is not unexpected, since the applicability of Vegard’s law has already
126 been observed for the lattice parameter of the four- and five-component
127 equimolar alloys within the Au-Cu-Ni-Pd-Pt-system [11]. This linear de-
128 pendency of the lattice parameter is a direct evidence for preserving the
129 single-phase fcc crystal structure throughout the entire compositional range.
130 Additionally, the scaling of the misfit parameter δ upon the composition is
131 shown in Fig. 2, which obviously is non-linear. It should be noted, that this
132 also holds for the dependency between δ and a . The lattice parameter of
133 AuNiPdPt ($a = 0.3875 \text{ nm}$) is slightly higher than the value obtained from
134 the rule of mixture of the constituent elements [11, 15]. These small differ-
135 ences do not change the predictions enough to account for the experimental
136 results.

137 Fig. 3 shows the interrelation of hardness and yield strength with the

138 composition of the $(\text{AuNiPdPt})_{1-x}\text{Cu}_x$ alloys. Both measures are not related
139 to each other. Nevertheless, the hardness is typically related to the flow stress
140 at a true plastic strain of 0.07 by a factor of ~ 3 [16]. The corresponding flow
141 stresses are also shown in Fig. 3, while selected true stress-strain curves
142 are provided in the supplementary. Summarising, the depicted values show
143 the same trend, i.e. a decrease with increasing Cu content. In particular,
144 the strength of this series apparently scales linearly with the concentration.
145 Furthermore, this linear scaling is also seen in dependence of the lattice
146 parameter (not shown here). The yield strength of AuNiPdPt amounts to
147 1308 MPa. This value is perplexingly high for a homogeneous solid solution
148 and would not have been expected when considering standard noble metal
149 based alloys as e.g. typically applied in jewellery.

150 Amongst the possible strengthening mechanisms in single-phase alloys,
151 the main contribution in this alloy series stems from solid solution strength-
152 ening ($\Delta\tau_{c,ss}$). This is because all samples are tested in a comparably coarse-
153 grained recrystallised state with low dislocation density. Therefore, Hall-
154 Petch-type strengthening ($\Delta\tau_{c,HP}$) as well as strain hardening ($\Delta\tau_{c,\rho}$) con-
155 tribute with a constant but low value to the total strength. In particular,
156 the contribution of grain boundary strengthening in AuCuNiPdPt amounts
157 to $\Delta\tau_{c,HP} = 23 - 33$ MPa for grain sizes ranging from 40 to 60 μm [12]. With
158 the plausible assumption that the Hall-Petch coefficient and the dislocation
159 density are similar for all alloys, the corresponding strengthening mechanism
160 do not affect the scaling behaviour significantly. In addition, no evidence
161 of long-range ordering was observed from transmission electron microscopy
162 utilising selected area electron diffraction for numerous zone axes (cf. supple-

163 mentary). Nevertheless, short-range ordering cannot be excluded from the
164 present experimental results.

165 Although, the yield strength is not supposed to show a linear scaling
166 with the misfit parameter, as shown in Fig. 4, the experimentally observed
167 behaviour cannot be explained exclusively by the misfit parameter as com-
168 monly seen for high-entropy alloys [17, 18, 19].

169 In particular, Varvenne et al. used their model in a reduced form, that
170 accounts only for elastic contributions to predict the yield strength of (no-
171 ble) high-entropy alloys, while the chemical contribution and solute/stacking
172 fault interaction energy is not considered [15]. The theory is valid if the dis-
173 location dissociation width $d > 6.5b$, and this depends on elastic constants
174 and stacking fault energy. This prerequisite might be violated in the Cu-
175 lean alloys due to the rather high stacking fault energies of the remaining
176 elements. A serious problem to experimentally prove these predictions lies
177 within the efforts to be done to obtain single-phase solid solutions from most
178 of these systems. Especially, those high-entropy alloys containing Ag turn
179 out to be difficult or even impossible to obtain single-phase. Other systems
180 possess miscibility gaps that might also be hard to overcome.

181 The most obvious contradiction between the experimental behaviour of
182 the yield strength and the corresponding calculations is the trend of the data.
183 While the yield strength is found to decrease with increasing Cu content (and
184 even with increasing misfit parameter) a non-linear increase of σ_y would be
185 expected from the model. Furthermore, it should be emphasised that the
186 absolute values as well as the spread across the Cu concentration of the
187 experimental yield strength are higher when compared to the theoretical

188 prediction with the exception of the AuCuNiPdPt alloy. It should be noted,
189 that the experimental values contain the friction stress ($\tau_0 \approx 39$ MPa) and
190 the contributions to the strength arising from grain boundaries ($\Delta\tau_{c,HP} \approx$
191 23 MPa) [12]. Considering the Taylor factor and the calculated $\Delta\tau_{c,ss}$ of the
192 AuCuNiPdPt alloy, the critical shear stress of $\tau_y = 268$ MPa (equivalent to
193 a yield strength of $\sigma_y = 820$ MPa) is well reproduced, i.e. $\tau_y = \tau_0 + \Delta\tau_{c,HP} +$
194 $\Delta\tau_{c,ss}$.

195 The calculations based on the proposed model for solid solution strength-
196 ening [1, 15] yield a maximum difference of only 14 MPa in strength for all
197 investigated alloys. Taking typical standard deviations for proof stresses into
198 account, the verification of this change is demanding and the change itself can
199 be considered negligible. In contrast, the mechanical tests performed reveal a
200 maximum yield strength of 1308 MPa in the case of AuNiPdPt and an almost
201 linear decrease of about 500 MPa towards AuNiCuPdPt. As the breakdown
202 of the scaling behaviour is obvious, the model might not be applicable with
203 the commonly applied simplifications being made. Furthermore, the experi-
204 mentally observed reduction in σ_y across the series of $(\text{AuNiPdPt})_{1-x}\text{Cu}_x$ is
205 large when compared to a slight variation of the calculated σ_y .

206 Recent experimental data on the room temperature hardness and yield
207 strength of single-phase, fcc $(\text{AuNiPdPt})_{1-x}\text{Cu}_x$ alloys were evaluated against
208 the model for solid solution strengthening in fcc high-entropy alloys [1, 9].
209 There is an obvious discrepancy between the experimental data and the
210 model as the strength decreases with increasing Cu content, while the model
211 predicts a slight increase. The observed difference cannot be rationalised in
212 terms of both absolute strength values and trend of strength with increasing

213 Cu content. While long range order could not be observed utilising TEM (cf.
214 supplementary), we cannot rule out short range order at present. It seems,
215 however, not likely because such an increase in strength can be observed for
216 some noble metals being optimised in strength by long range order [20] but
217 the strength increase of short range order is expected to be lower. Otherwise,
218 the model assumes that the shear modulus of the alloys can be calculated
219 upon the rule of mixture, which might not be true. Further investigations are
220 required to resolve these open questions. For now, it is questionable whether
221 the model that assumes a random matrix and additional solutes involving
222 solely an averaged shear modulus is capable of accurately describing solid
223 solution strengthening in the present case. The evaluation of further high-
224 entropy alloy series and the stacking fault energy variation within the present
225 system are required to address this open question.

226 Funding: This work was supported by the Deutsche Forschungsgemein-
227 schaft (DFG) within the priority programme *Compositionally Complex Alloys*
228 - *High Entropy Alloys (CCA-HEA)* (SPP 2006, grants no. FR 1714/7-1 (FT,
229 JF) and STU 611/2-1 (DU, KA)). Furthermore, we would like to express our
230 gratitude to D. Seifert, S. Donat, C. Damm, C. Bollnow and B. Gebel for
231 experimental support.

232 References

- 233 [1] C. Varvenne, A. Luque, W. A. Curtin, *Acta Mater.* 118 (2016) 164–176.
234 doi:10.1016/j.actamat.2016.07.040.
- 235 [2] B. Cantor, I. Chang, P. Knight, A. Vincent, *Mat. Sci. Eng. A* 375–
236 377 (C) (2004) 213–218. doi:10.1016/j.msea.2003.10.257.

- 237 [3] J.-W. Yeh, S.-K. Chen, S.-J. Lin, J.-Y. Gan, T.-S. Chin, T.-T. Shun,
238 C.-H. Tsau, S.-Y. Chang, *Adv. Eng. Mater.* 6 (5) (2004) 299–303.
239 doi:10.1002/adem.200300567.
- 240 [4] E. P. George, D. Raabe, R. O. Ritchie, *Nat. Rev. Mater.* 4 (2019) 515–
241 534. doi:10.1038/s41578-019-0121-4.
- 242 [5] E. George, W. Curtin, C. Tasan, *Acta Mater.* (2019) in press-
243 doi:10.1016/j.actamat.2019.12.015.
- 244 [6] Deutsche Forschungs Gemeinschaft, information für die Wissenschaft
245 Nr. 65 (2016). [link].
246 URL [https://www.dfg.de/foerderung/info_wissenschaft/2016/info_wissenschaft_16.](https://www.dfg.de/foerderung/info_wissenschaft/2016/info_wissenschaft_16)
- 247 [7] R. Labusch, *Phys. Stat. Sol. B* 41 (1970) 659–669.
248 doi:<https://doi.org/10.1002/pssb.19700410221>.
- 249 [8] I. Toda-Caraballo, P. Rivera-Diaz-del Castillo, *Acta Mater.* 85 (2015)
250 14–23. doi:10.1016/j.actamat.2014.11.014.
- 251 [9] C. Varvenne, G. P. M. Leyson, M. Ghazisaeidi, W. A. Curtin, *Acta*
252 *Materialia* (2017) 660–683doi:10.1016/j.actamat.2016.09.046.
- 253 [10] W. Nöhring, W. Curtin, *Scripta Mater.* 168 (2019) 119–123.
254 doi:10.1016/j.scriptamat.2019.04.012.
- 255 [11] J. Freudenberger, D. Rafaja, D. Geissler, L. Giebeler, C. Ullrich,
256 A. Kauffmann, M. Heilmaier, K. Nielsch, *Metals* 7 (4) (2017) 135.
257 doi:10.3390/met7040135.

- 258 [12] F. Thiel, D. Geissler, K. Nielsch, A. Kauffmann, S. Seils, M. Heilmaier,
259 D. Utt, K. Albe, M. Motylenko, D. Rafaja, J. Freudenberger, *Acta*
260 *Mater.* 185 (2020) 400–411. doi:10.1016/j.actamat.2019.12.020.
- 261 [13] C. Varvenne, A. Luque, W. Nöhring, W. Curtin, *Phys. Rev. B* 93 (2016)
262 104201. doi:10.1103/physrevb.93.104201.
- 263 [14] C. R. LaRosa, M. Shih, C. Varvenne, M. Ghazisaeidi, *Mater. Char.* 151
264 (2019) 310–317. doi:10.1016/j.matchar.2019.02.034.
- 265 [15] C. Varvenne, W. Curtin, *Scripta Mater.* 142 (2018) 92–95.
266 doi:10.1016/j.scriptamat.2017.08.030.
- 267 [16] K. L. Johnson, *Contact Mechanics*, Cambridge University Press, 1985.
- 268 [17] G. Bracq, M. Laurent-Brocq, C. Varvenne, L. Perriere, W. Curtin,
269 J.-M. Joubert, I. Guillot, *Acta Mater.* 177 (2019) 266–279.
270 doi:10.1016/j.actamat.2019.06.050.
- 271 [18] S. Yoshida, T. Ikeuchi, T. Bhattacharjee, Y. Bai, A. Shibata, N. Tsuji,
272 *Acta Mater.* 171 (2019) 201–215. doi:10.1016/j.actamat.2019.04.017.
- 273 [19] B. Yin, W. A. Curtin, *npj Comput. Mater.* 5 (2019) 14.
274 doi:10.1038/s41524-019-0151-x.
- 275 [20] B. Greenberg, N. Kruglikov, L. Rodionova, A. Volkov, L. Grokhovskaya,
276 G. Gushchin, I. Sakhanskaya, *Platin. Met. Rev.* 47 (2003) 46–58.

Table 1: Input data of the properties for the pure elements contained in the HEA taken from the “Springer Handbook of Materials Data”. a_0 is the fcc lattice constant, E the Young’s modulus, and G the shear modulus.

Element	$a_0/\text{\AA}$	G/GPa	E/GPa
Au	4.0784	26	78
Cu	3.6149	46.8	128.8
Ni	3.5241	78.5	220
Pd	3.8901	43.5	121
Pt	3.9233	60.9	170

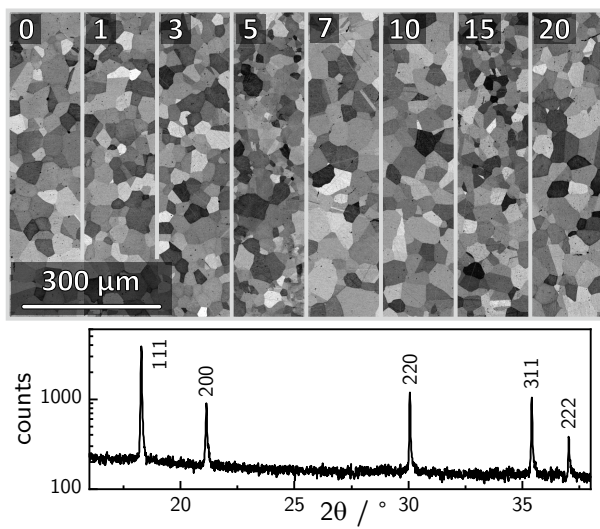


Figure 1: Microstructure of $(\text{AuNiPdPt})_{1-x}\text{Cu}_x$ alloys in the recrystallised state. The scaling bar accounts for all micrographs and the depicted number accounts for the Cu content. The lower part of the image shows the XRD pattern for $x = 3$ as a representative example of this series.

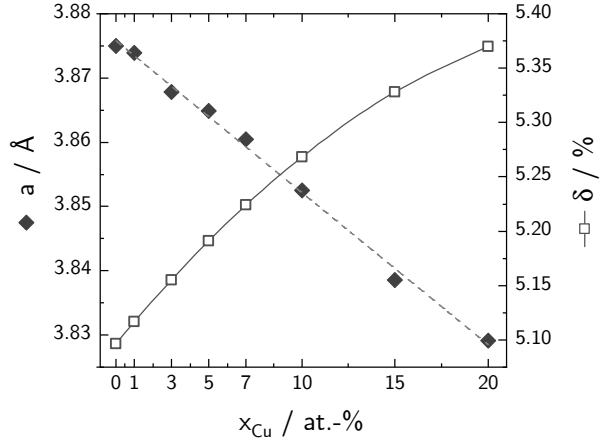


Figure 2: Lattice parameter of $(\text{AuNiPdPt})_{1-x}\text{Cu}_x$ alloys (closed symbols, linear trend) as well as misfit parameter δ (open symbols, non-linear trend) in dependence of the Cu content. The lines are guides to the eye, only.

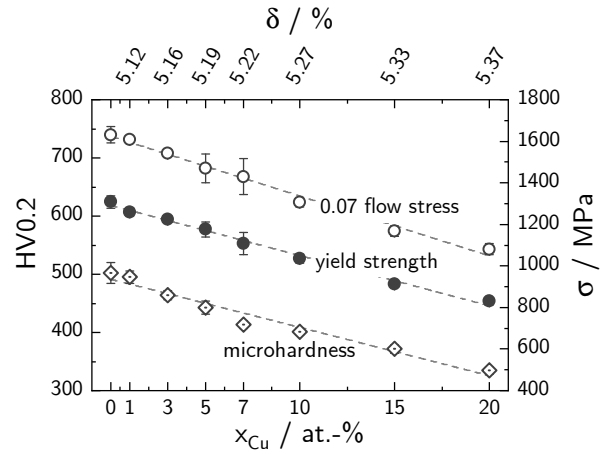


Figure 3: Vickers microhardness (\diamond), yield strength (\bullet) and flow stress at 0.07 plastic strain (\circ) of $(\text{AuNiPdPt})_{1-x}\text{Cu}_x$ alloys in dependence of the Cu content. The upper labels refer to the misfit parameter δ for the depicted composition. The dashed lines represent linear fits to the data.

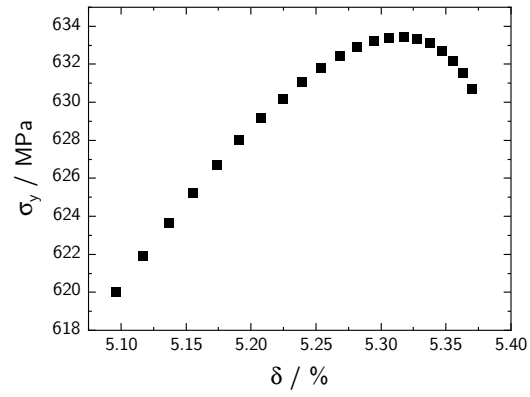


Figure 4: Calculated yield strength as a function of the misfit parameter in accordance to the Varvenne model [1].